Development of a capillary zone electrophoresis method to quantify E. coli L-asparaginase and its acidic variants

Yao, Han; Vandenbossche, Jana; Sänger-van de Griend, Cari E.; Janssens, Yorick; Fernández, Cristina Soto; Xu, Xiaolong; Wynendaele, Evelien; Somsen, Govert Willem; Haselberg, Rob; De Spiegeleer, Bart

published in
Talanta
2018

DOI (link to publisher)
10.1016/j.talanta.2018.01.048

document version
Publisher's PDF, also known as Version of record

Talanta 182 (2018) 83–91

Contents lists available at ScienceDirect

Talanta

journal homepage: www.elsevier.com/locate/talanta

Development of a capillary zone electrophoresis method to quantify *E. coli* L-asparaginase and its acidic variants

Han Yao[a], Jana Vandenbossche[a], Cari E. Sänger-van de Griend[b], Yorick Janssens[a], Cristina Soto Fernández[a], Xiaolong Xu[a], Evelien Wynendaele[a], Govert Willem Somsen[c], Rob Haselberg[c], Bart De Spiegeleer[a,*]

[a] Drug Quality and Registration (DruQuaR) Group, Department of Pharmaceutical Analysis, Faculty of Pharmaceutical Sciences, Ghent University, Ottergemsesteenweg 460, 9000 Ghent, Belgium

[b] Division of Analytical Pharmaceutical Chemistry, Faculty of Pharmacy, Department of Medicinal Chemistry, Uppsala University, Biomedical Centre, PO Box 574, SE-751 23 Uppsala, Sweden

[c] Division of BioAnalytical Chemistry, AIMMS Research Group BioMolecular Analysis, Vrije Universiteit Amsterdam, De Boelelaan 1085, 1081 HV, Amsterdam, The Netherlands

ARTICLE INFO

Keywords:
l-asparaginase
Capillary zone electrophoresis
Acidic impurities
Design of experiments (DoE)

ABSTRACT

A capillary zone electrophoresis (CZE) method with UV detection was developed for the quantification of the *E.coli* L-asparaginase (L-ASNase) and its acidic variants. During the initial method development, a variety of experimental conditions were screened. Subsequently, a Design of Experiments (DoE) was used to optimize the pH and concentration of the selected background electrolyte (BGE) containing both TRIS and boric acid. Optimization was performed taking into account both the separation efficiency of L-ASNase and its acidic variants as well as overall method robustness. A repeatable separation between *E.coli* L-ASNase and its acidic variants was achieved on a bare fused silica capillary in combination with a BGE consisting of both 400 mM TRIS and boric acid. The method was validated for linearity, accuracy, precision, LOD, LOQ and robustness. The recovery for L-ASNase was 97.9–104.4% with a precision RSD of 1.5–3.2%, while the recovery of impurities was 92.1–109.8% with a RSD of 1.7–4.6%. The quantification limit was 1.9% (m/m). Moreover, the CZE-UV method was applied to determine the degradation rate in the presence of ammonium bicarbonate, confirming the suitability of the method. The degraded, partially charged L-ASNase was evaluated for its *in-vitro* enzymatic activity showing an insignificant different enzyme activity compared to the unmodified sample.

1. Introduction

L-asparaginase (L-ASNase) is a tetrameric enzyme used in pediatric treatment of acute lymphoblastic leukaemia (ALL) [1]. Clinically used L-ASNase preparations are currently derived from two bacterial sources: *Escherichia coli* and *Erwinia chrysanthemi* [1], with a tetrameric molecular weight (MW) of 136,320 Da resp. 140,320 Da and an isoelectric point (pI) of 4.9 resp. 8.6 [2–4]. Like other biopharmaceuticals, L-ASNase is prone to modifications during its bacterial production as well as pharmaceutical processing and storage [5]. Also, during the preclinical and clinical trials, consistency in the nature and quantity of these modifications is of critical importance for a successful development of the originator medicines as well as of the biosimilars. The consistency of these modifications is also crucial for the novel L- ASNase formulations under development [6,7]. As these protein modifications are known to change the physicochemical, immunochemical, biological and pharmacological properties, which may contribute to adverse effects, it is important to characterize this heterogeneity [8].

Charge variants are an important type of protein heterogeneity and typically consist of acidic variants (*e.g.* sialylation and deamidation) and basic variants (*e.g.* succinimide formation and oxidation of some amino acid side chains [Met, Cys, Lys, His, Trp] and C-terminal Lys cleavage) [6,9]. Deamidation is one of the most frequent acidic degradation pathways and is common in Asn residues [10]. The Asn deamidation reaction results in a cyclic succinimide, which is further hydrolysed to form an Asp and isoAsp mixture (with a mass increase of 1 Da from 114 Da for Asn to 115 Da for Asp) with the release of ammonia [10]. This leads to a decrease of the isoelectric point (pI) due to the change in residue charge from neutral to the acidic carboxylate. Moreover, deamidation generally leads to loss of biological function, secondary and tertiary structure and stability [11,12]. However, deamidated variants of *Erwinia* L-ASNase (deamidated site: Asn281) are

* Corresponding author.
E-mail address: Bart.DeSpiegeleer@UGent.be (B. De Spiegeleer).

https://doi.org/10.1016/j.talanta.2018.01.048
Received 7 November 2017; Received in revised form 14 January 2018; Accepted 17 January 2018
Available online 20 February 2018

reported to retain their *in-vitro* enzymatic activity [13]. No studies concerning about the enzyme activity of the deamidated variants of *E.coli* L-ASNase have been reported yet. Charge variants of proteins can be analyzed using a variety of techniques for distinct purposes, including isoelectric focusing like slab gel isoelectric focusing (IEF) and capillary isoelectric focusing (CIEF), capillary electrophoresis, ion-exchange chromatography (IEX), and mass spectrometric techniques [14–26]. A traditional method for evaluating the charge variants is the IEF [14,15]. IEF can provide high-resolution separation of similar charge variants, but it is time consuming, labor intensive and has an unsatisfactory quantitation precision. Other techniques reported were CIEF [14–17] and more recently imaged capillary electrophoresis (iCE) [18,19]. However, while they allow more quantitative evaluation, these techniques are still time consuming. Capillary zone electrophoresis (CZE) has recently been shown to be a suitable technique to characterize protein charge variants due to its high resolution and speed, low sample consumption and low cost availability of capillaries [20–22]. The charge variants of *Erwinia* L-ASNase, such as the deamidated variants and the non-deamidated acidic variants, have been characterized in the recent years by using IEX, CIEF, liquid chromatography tandem-mass spectrometry (LC-MS/MS) of proteolytic digests, and structural techniques including circular dichroism (CD), small-angle X-ray scattering (SAXS) and ion-mobility mass spectrometry (IM-MS) [25–29]. The charge variants of *E.coli* L-ASNase has been much less studied compared to that of *Erwinia* L-ASNase; some investigations have been reported such as the characterization of succinylated charge variants by using ultraviolet spectroscopy, fluorescence spectroscopy and CD, and the identification of deamidated variants by LC-MS/MS of proteolytic digests [25,30]. Regarding to the CZE-UV method, up till now, only one CZE-UV method for *Erwinia* L-ASNase is briefly reported without analytical details [13]. Moreover, the acidic variants were not separated. No CZE-UV methods for determining *E.coli* L-ASNase and charge variants have ever been reported.

In this study, a systematic development of a CZE-UV method for the quantification of L-ASNase as well as of the acidic variants of *E.coli* L-ASNase is presented. After an initial screening investigation, the method was optimized using experimental designs (DoE) following the quality-by-design (QbD) concept to define the design space. The optimized method was further formally validated and applied on different deamidated L-ASNase samples, which were finally evaluated for their functional enzyme activity.

2. Experimental

2.1. Materials

Hydrochloric acid, TRIS (Trizma®base), boric acid, sodium hydroxide, ammonium bicarbonate, potassium iodide, mercury (II) iodide and trichloroacetic acid (TCA) were purchased from Sigma-Aldrich (St. Louis, Missouri, USA). Potassium phosphate monobasic and L-asparagine monohydrate were obtained from Merck (Darmstadt, Germany). Ammonium chloride was purchased from UCB (Brussels, Belgium). All chemicals were analytical grade. Paronal® samples, *i.e. E.coli* L-ASNase preparation without excipients (label claim of 10,000 IU per vial; Kyowa Hakko Kiri Co., Ltd.) (Tokyo, Japan), were obtained from Takeda Pharmaceutical Co., Ltd. (Brussels, Belgium). In the absence of a formal reference standard for the selective assay of L-ASNase, batch 10858381 was used as laboratory reference material, which contained 79.1% of active pharmaceutical ingredient (API), 14.4% of impurity 1, 4.5% of impurity 2% and 2.0% of impurity 3, based on peak deconvolution and area normalization (see Section 2.5) [31–33].

2.2. Sample and BGE preparation

For the initial development and the following optimization, 1 mg/mL L-ASNase in water was applied. In the initial development, BGEs of 500 mM/500 mM, 600 mM/600 mM and 800 mM/800 mM TRIS/boric acid at different pH values (pH 7.5, pH 8.0, pH 8.5, pH 8.25, pH 8.75 and pH 9.5), and 1 M/1 M TRIS/boric acid (pH 8.5 and pH 8.0) were prepared. Moreover, potassium tetraborate solution at fixed concentration of 50 mM (pH 7.0, pH 8.0, pH 9.0 and pH 10.0), boric acid solution (50 mM, adjusted to pH 10), and TRIS solution (25 mM, pH 8.0) and (50 mM, pH 8.0) were prepared. Additionally, 200 mM/200 mM TRIS/tricine (pH 8.24) was also prepared. All above BGEs were tested on the bare fused-silica capillary. In the entire study, 1 M hydrochloric acid or 1 M sodium hydroxide was applied, when the pH adjustment is required.

Regarding the method optimization, a three level central composite design (CCD) with three center points is employed to define the design space of the pH and concentration of BGE (Supplementary material Table 1) [34]. Each experimental block consisting of 11 runs, was performed in triplicate. The factors and their ranges were 1) concentration of TRIS/boric acid ranging from 100 mM/100–600 mM/600 mM, 2) pH of TRIS/boric acid ranging from pH 8.0 to pH 9.0. For these experiments, 100 mM/100 mM TRIS/boric acid (pH 8, pH 8.5 and pH 9), 350 mM/350 mM TRIS/boric acid (pH 8, pH 8.5 and pH 9) and 600 mM/600 mM TRIS/boric acid (pH 8, pH 8.5 and pH 9) were applied. For the final method, the running BGE consisted of 400 mM TRIS and 400 mM boric acid (pH unadjusted, the measured pH value was pH 8.4).

The final method was applied on different modified (degraded) samples to test the modification rate. 1.0 mg/mL L-ASNase samples were stored in 1% NH_4HCO_3 (m/v), and incubated at 37 °C for 0, 8, 16 and 24 h [13,35].

2.3. CE parameters

Proteomelab PA 800 plus CE instrument (Beckman Coulter, Brea, United States) was used coupled with a diode array detector. In the method development and validation parts, a bare fused-silica capillary (Polymicro Technologies, Phoenix, AZ, USA) was used which possessed an effective length of 20 cm and internal diameter of 50 µm (outer diameter, 365 µm). Samples were kept at a temperature of 10 °C and injected at 0.4 psi for 4 s. The separation voltage was 9 kV, and the polarity was normal. UV absorbance was detected at 214 nm and the optical window was 200 µm. New fused silica capillaries were pretreated with 1 M NaOH, water, and BGE subsequently at 20 psi for 20 min. Between two consecutive injections, the fused silica capillary was flushed with 1 M NaOH, water and BGE for 2 min at 20 psi, respectively.

2.4. Method characteristics

2.4.1. Relative response factor of the acidic L-ASNase species

Neglecting differences in MW of the unmodified L-ASNase and the acidic species (*i.e.* amide *versus* acid), the relative response factor (RRF) of the acidic species relative to the unmodified L-ASNase is defined by [36]:

$$RRF = \frac{\text{area of acidic species}}{(\text{original area of unmodified L-ASNase}) - (\text{residual area of unmodified L-ASNase in modified sample})}$$

As quantitative evaluation of these related impurities can be accomplished using the internal normalization procedure, the raw data (*i.e.* peak area or height) are to be converted to mass units (*i.e.* as %). Therefore, the relative response factor (RRF) needs to be assessed: if this RRF falls between 0.80 and 1.20, then no consideration for it is normally required (*i.e.* an RRF of 1.0 can be used). In the absence of

appropriate reference standards for these impurities, and using mass and peak balance principles, an estimation of RRF (in UV 214 nm) can be obtained using unstressed and stressed (degraded) solutions, as demonstrated in [36].

2.4.2. Selectivity

The modified L-ASNase sample was prepared by incubating 2.0 mg/mL L-ASNase in 1% NH_4HCO_3 at 37 °C for 48 h. The sample was contained in the 2 mL Eppendorf tube and the temperature was controlled by the oven (Binder; Bohemia, USA). The selectivity was evaluated by the separation (expressed as peak to valley ratio [p/v]) between the API and the acidic impurities in modified L-ASNase sample. The p/v is the ratio between the peak height of impurity 1 and the valley between API and impurity 1, defined according to the Ph. Eur [37]. The definition of impurity 1 can be found in Section 3.1.

2.4.3. Linearity and range

Regarding L-ASNase, 2.5 mg reference material (corresponding to 1.98 mg/mL API, seen the impurities present) was dissolved in 1.0 mL of water. 20.0, 40.0, 80.0 and 120.0 µL of above solution were diluted to 200.0 µL to obtain final concentrations representing 25% (0.198 mg/mL), 50% (0.396 mg/mL), 100% (0.791 mg/mL) and 150% (1.187 mg/mL) of L-ASNase concentration of 0.791 mg/mL. For impurity 1, 27.3, 54.3, 108.8, 163.0 and 326.0 µL of the 2.0 mg/mL modified L-ASNase solution was diluted to 500.0 µL to obtain final concentrations representing 0.036, 0.072, 0.144, 0.215 and 0.430 mg/mL of impurity 1. Concerning impurity 2, 21.7, 32.6, 43.4, 65.1 and 130.2 µL of the 2.0 mg/mL modified L-ASNase solution was diluted to 500 µL to obtain final concentrations representing 0.022, 0.034, 0.045, 0.068 and 0.135 mg/mL of impurity 2.

2.4.4. Accuracy and precision

The recovery is calculated as the ratio between the concentration found and the theoretical concentration. The concentration found is calculated by fitting the obtained peak area values in the equation of the calibration curve. The preparation of these solutions (each concentration in triplicate) is the same as in Section 2.4.3: with respect to L-ASNase, three reference solutions representing 0.396, 0.791 and 1.187 mg/mL of L-ASNase reference solution were used. For impurity 1 and impurity 2, the 2.0 mg/mL modified L-ASNase solutions representing 0.072, 0.144 and 0.215 mg/mL of impurity 1 and 0.034, 0.045 and 0.068 mg/mL of impurity 2 were used respectively.

2.4.5. LOD and LOQ

For determining the LOD/LOQ of L-ASNase, the 0.198 mg/mL L-ASNase reference solution was used. Concerning impurity 1 and impurity 2, the 2.0 mg/mL modified L-ASNase solutions representing 0.036 mg/mL of impurity 1 and 0.022 mg/mL of impurity 2 were used (see Section 2.4.3.). Signal is defined as the height of the compounds peak. Noise is defined as the difference between the highest and lowest values of the baseline, observed over a distance equal to 5 times the width at the half-height of the compound peak, situated in the area after the compound peak.

2.4.6. Robustness evaluation

A three level Plackett-Burman design (PBD) with three center points was adopted to test the robustness of the applied final method (Supplementary material Table 2) [38]. The factors were defined as the pH of BGE ranging between 8.30 and 8.50 and the concentration of BGE ranging between 395 and 405 mM.

2.5. Data analysis

For the DoE, the set-ups and their evaluations were performed by MODDE 8.0.2 software from Umetrics (Umea, Sweden). In order to quantify the overlapping peaks, peak deconvolution was applied, using Gaussian peak algorithm (deconvolution filter of 75; vary peak width) (PeakFit V4 software; Chicago, United States).

2.6. Enzyme activity of the modified L-ASNase

The functional enzyme activity of the modified L-ASNase samples (see Section 2.2) was investigated using a previously developed Nessler method [39]. 1.0 mL of each 1.0 mg/mL (250 IU/mL, one 10,000 IU vial L-ASNase contains 40 mg powder) sample was further diluted to 50.0 mL using phosphate buffer pH 7.4 (prepared by using a 0.2 M potassium dihydrogen phosphate and 0.1 M sodium hydroxide), yielding a theoretical 5 IU/mL solution. To 0.1 mL of this solution, 1.9 mL of 20 mM L-Asn (ligand solution) was added. This reaction was carried out at 37 °C for 15 min and stopped by addition of 0.5 mL of 25% TCA. Ammonium chloride solution (50 ppm) was employed as reference solution. After the reaction with the Nessler reagent, the absorbance of the sample and reference solution at 450 nm was further measured as previously reported [39]. Samples were analyzed in duplicate.

3. Results

3.1. Initial method development

In the initial development, a bare capillary (effective length of 20 cm; internal diameter of 50 µm) was tested, in order to achieve a CE-UV method possessing high resolution, short migration time and good peak shape. Both the low ionic strength BGEs, *i.e.* potassium tetraborate (50 mM, pH 7.0–10.0), boric acid (50 mM, pH 10), and TRIS (25 mM, pH 8.0; 50 mM, pH 8.0) and high ionic strength buffers, *i.e.* 200 mM/200 mM TRIS/tricine (pH 8.24) and 500 mM/500 mM TRIS/boric acid (pH 8.5), were investigated on this bare fused-silica capillary. These BGEs were chosen due to their simplicity and the p*K*a of BGEs components. The pH of BGEs is at least one unit higher than the pI (4.9) of *E.coli* L-ASNase [4]. Overall, on the bare fused-silica capillary, only the BGE of TRIS/boric acid could separate the API from its charge impurities, and hence was used for further investigation.

The influence of the concentration and pH of the TRIS/boric acid was further explored on the bare fused-silica capillary, within a concentration range from 500 mM/500–800 mM/800 mM and a pH range from 8.0 to 9.0. Since the pI (4.9) of native *E.coli* L-ASNase is under these BGE pH (8.0–9.0), the acidic variants will be more negatively charged. Thus, the acidic variants will show a longer migration time, compared to the native L-ASNase, as observed in Fig. 1**a**. The acidic impurity closest to the API peak is defined as impurity 1. Increasing the BGE concentration leads to an improved p/v, going from 1.18 (500 mM/500 mM) to 1.32 (800 mM/800 mM), but increases also the run time. pH increase leads to shorter migration times, but a lower p/v, varying from 1.41 (pH 8.0) to 1.18 (pH 8.75) (Fig. 1**b**). The resolution is defined as peak to valley ratio (p/v) *i.e.* the ratio between the peak height of impurity 1 and the valley between API and impurity 1. Considering the benefits and drawbacks, the concentration and pH of BGE were further systematically investigated by using DoE.

Moreover, other CE parameters were also investigated on the bare fused-silica capillary, with 600 mM TRIS/600 mM boric acid (pH 8.25) as BGE. Capillary effective lengths of 40 cm, 20 cm and 10 cm were tested: a sufficiently shorter migration time (maximum 10 min) as well as a sufficient p/v (minimum 1.3) can be obtained on the effective 20 cm length capillary, which was chosen as the final length. Different separation voltages (*i.e.* 9, 14, 18, 23, 27 and 30 kV) were tested: since higher voltages lead to a worse separation, 9 kV was therefore selected. Cartridge temperature, *i.e.* 15 and 25 °C, and the optical window, *i.e.* 200 and 800 µm, leads to similar migration times and peak separations. Therefore, a lower cartridge temperature of 15 °C and a narrow optical window of 200 µm was chosen.

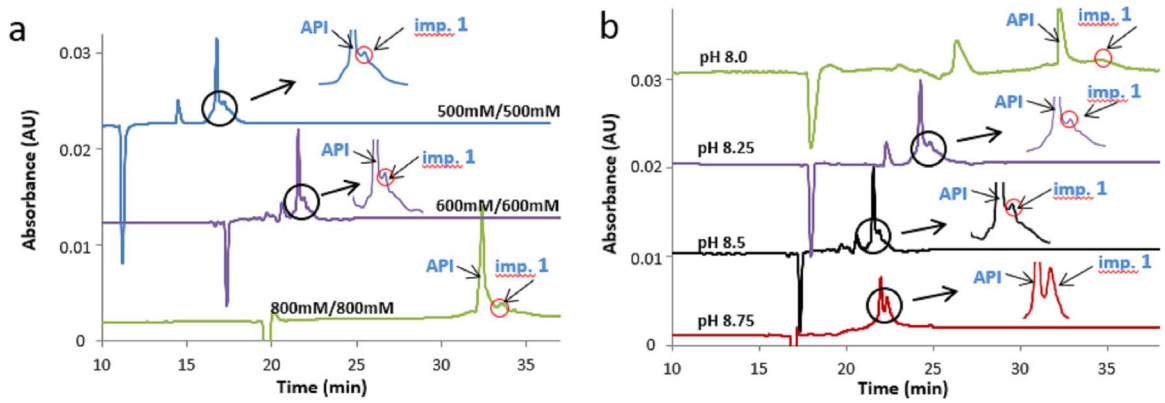

Fig. 1. Electropherograms of 1.0 mg/mL L-asparaginase preparation: a) 500 mM/500 mM, 600 mM/600 mM and 800 mM/800 mM TRIS/boric acid of pH 8.5. API is overlaid with the system peak under the condition of 800 mM/800 mM TRIS/boric acid (pH 8.5); b) pH 8.0, pH 8.25, pH 8.5 and pH 8.75 TRIS/boric acid of concentration 600 mM/600 mM. Impurity 1 is overlaid with the system peak under the condition of 600 mM/600 mM TRIS/boric acid, pH 8.75. Imp.1 stands for impurity 1.

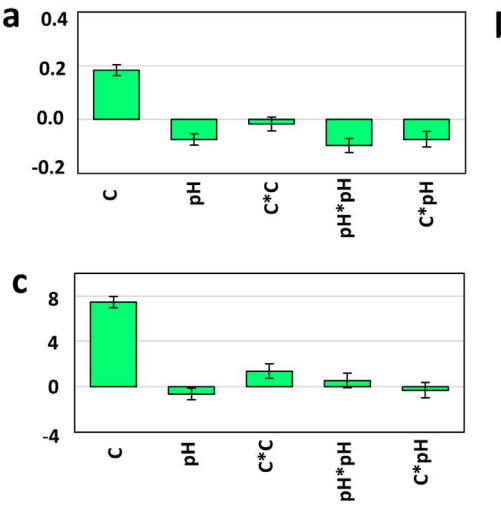

Fig. 2. Regression coefficients of central composite design: a) response 1, peak to valley ratio; b) response 2, RSD of peak area of API; c) response 3, migration time of API.

3.2. Method optimization using a QbD philosophy

3.2.1. Critical method attributes (CMAs) and critical method variables (CMVs)

Design of experiments (DoE), as a key aspect of quality by design (QbD), is a well-proven characterization approach within analytical method development. The purpose is to investigate the individual and combined effects of CMVs on CMAs. According to the observation in the initial method development, concentration of BGE and pH are chosen as the critical method variables (CMVs). CMAs are important method characteristics defined here as: 1) resolution expressed as the peak to valley ratio between the API and the closest impurity (max); 2) RSD (%) of migration time of API (min); 3) RSD (%) of peak area of API (min); 4) migration time of API (min).

3.2.2. Determination of the design space

The primary purpose of the full CCD was to define the design space where a high resolution, a short and robust migration time, and a robust peak area can be obtained. By applying multivariate regression analysis, a fitted full second order model was obtained for the four responses, given by the following equation:

$$Y = \beta_0 + \beta_1 X_1 + \beta_2 X_2 + \beta_{11} X_1^2 + \beta_{22} X_2^2 + \beta_{12} X_1 X_2$$

where, Y: the response; β_0: the intercept; β_1, β_2: regression coefficients of the factors X_1 (concentration) and X_2 (pH), respectively.

The relationships between the factors and the different responses are elucidated by regression analysis and indicated by the coefficients of the regression models. For the peak to valley ratio as response, shown in Fig. 2**a** and Supplementary material Table 3, concentration, pH, and pH*pH and C*pH were the significant factors: concentration is able to significantly increase the response of p/v ratio, while pH, pH*pH and C*pH have a significantly inverse relationship with the p/v ratio. Analysis of variance (ANOVA) indicated that the model was statistically significant in its prediction property of the response p/v, as depicted by a Q^2 value of 0.94 (goodness of prediction). The difference (0.05) between R^2 and Q^2 is smaller than 0.2, suggesting that the overall model fits well [40]. Moreover, pH and pH* pH were found to be the significant factors for the response RSD of peak area of the API, while C and C*C were the significant factors for migration time of API (Fig. 2**b-c**). However, the response RSD of migration time does not fit regression model, due to its insufficient prediction ability (Q^2, − 0.2) and reproducibility value of 0.44 (*e.g.* a numerical summary of the variability with a limit of 0.5) [40].

In a DoE strategy, the design space is considered as a zone of robustness: no drastic changes in analytical characteristics will occur when working within the design space. The target specifications of the responses are defined to be: the p/v ratio, as large as possible (minimum 1.3); the response of RSD peak area, as small as possible (maximum 4.0); migration time, as short as possible (maximum 16 min). In order to define the design space, contour plots were analyzed to visualize the individual and combined effects of BGE concentration and pH on the responses (Fig. 3**a-c**). A sweet spot plot was adopted, which is an overlay of several response contour plots, showing how many of the specification criteria are fulfilled (Fig. 3**d**). In the

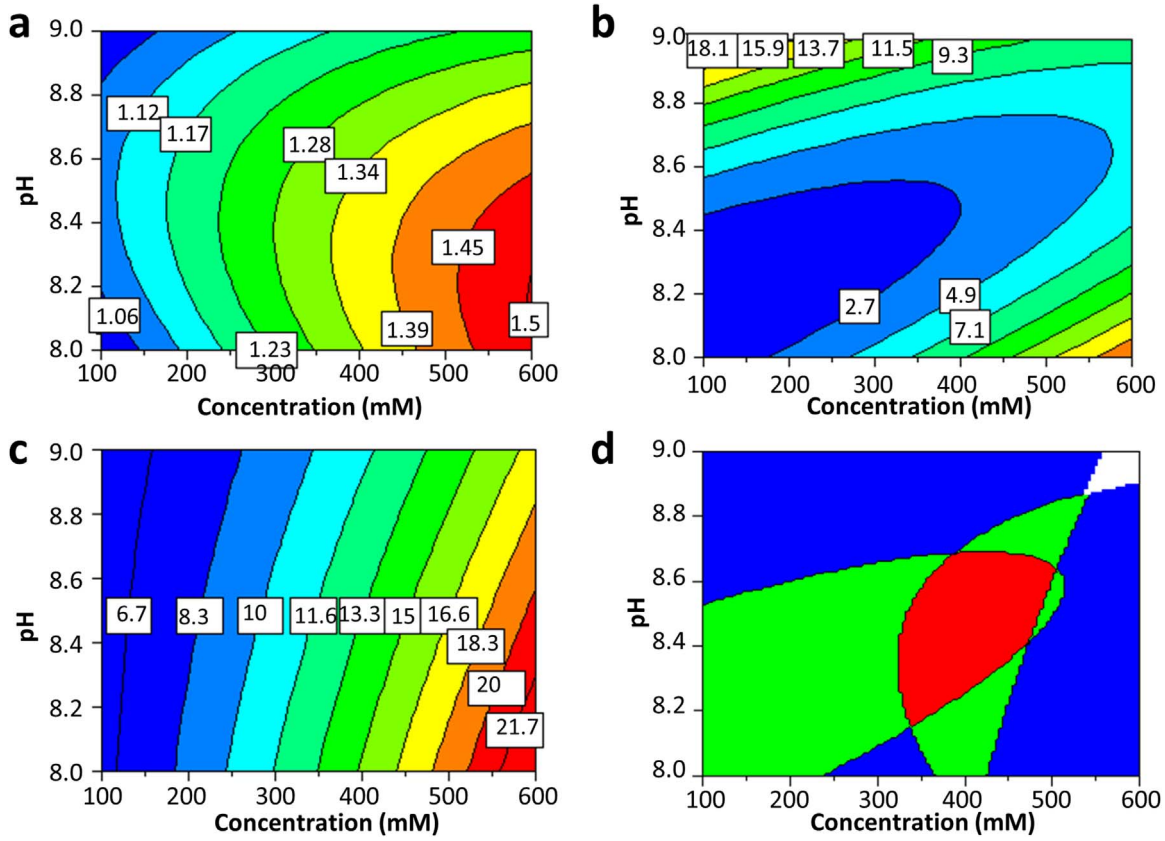

Fig. 3. Response surface (2D) contour plots showing the effects of concentration (C) and pH on the three responses: a) peak to valley ratio; b) RSD of peak area of API; c) migration time (min) of API; d) sweet spot of above three responses in red. (For interpretation of the references to color in this figure legend, the reader is referred to the web version of this article.)

white, blue and green spaces, no, one or two criteria are fulfilled respectively. The red space represents the sweet plot where all three criteria are fulfilled, equivalent to the QbD design space (Fig. 3**d**). Therefore, we could define the combined design space: the BGE concentration ranging between 350 mM and 450 mM (for both TRIS/boric acid) while the pH ranging between 8.3 and 8.5. An optimal point with a concentration of 400 mM and a pH of 8.4 is proposed, which is the middle point of the design space.

3.3. Method validation

3.3.1. Relative response factor of the acidic L-ASNase species

The mean RRF of the acidic species was calculated to be 1.01 ± 0.02 (mean ± SD, n = 2), using the 2 mg/mL modified L-ASNase sample obtained by incubating in 1% NH_4HCO_3 at 37 °C for 48 h. Therefore, the factor correction is not required for the validation tests of impurity 1 and impurity 2, since the API and the impurities showed a similar UV response. Using area normalization, 0.664 mg/mL of impurity 1 and 0.516 mg/mL of impurity 2 were determined in the 2 mg/mL modified sample, which is further used for the validation of impurity 1 and impurity 2. The peak observed at 9 min is a system peak, which is also observed in the blank. Since L-ASNase and the impurities show similar the DAD spectra (Fig. 4), the peak purity can not be determined by using these DAD spectra.

3.3.2. Validation results

For the selectivity, the acidic impurities 1, 2 and 3 are separated from the API in the modified L-asparaginase (Fig. 4).

The calibration curves were found linear over a concentration range of 0.20–1.98 mg/mL for L-ASNase, 0.036–0.430 mg/mL for impurity 1 and 0.023–0.135 for impurity 2. The impurity 3 is not validated, due to its low amount (2.0%, see Section 2.1) in the native sample. The

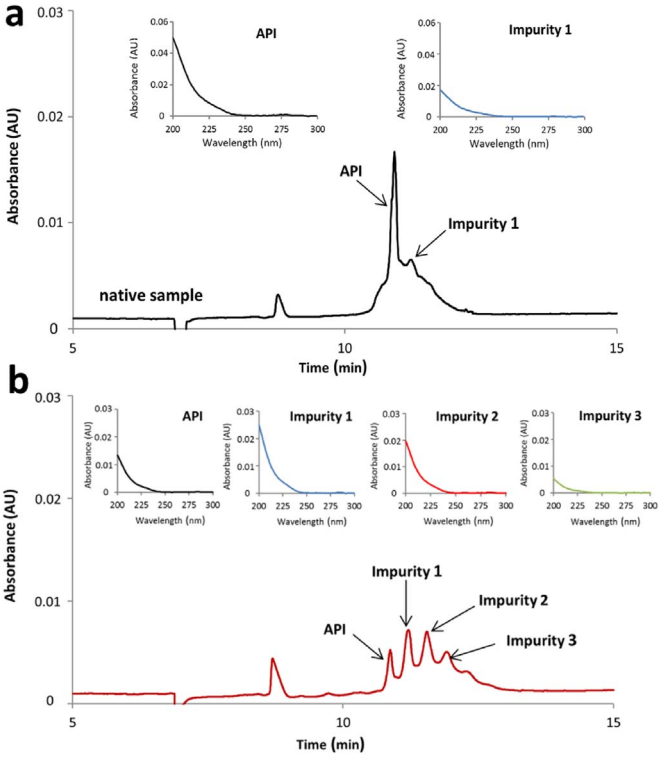

Fig. 4. Electropherograms of 2.0 mg/mL native L-asparaginase (a) and 2.0 mg/mL modified L-asparaginase (b). BGE consisting of 400 mM TRIS and 400 mM boric acid (pH unadjusted, the measured pH value was pH 8.4) is applied. a: the inserted DAD spectra (200–300 nm) obtained at the apex of the L-ASNase and impurity 1 CE-UV peaks from the native L-ASNase. b: the inserted DAD spectra (200–300 nm) obtained at the apex of the L-ASNase and impurity 1–3 CE-UV peaks from the modified L-ASNase.

Table 1
Calibration linearity and range.

Compound	Range (mg/mL)	Slope	Intercept	R-squared
L-ASNase	0.20–1.98	2169 [1984–2354][a]	− 151.7 [− 356.7 to 53.4][b]	0.9978
Impurity 1	0.036–0.430	2329 [2036–2622][a]	− 52.0 [− 119.4 to 15.3][b]	0.9953
Impurity 2	0.023–0.135	1576 [1304–1849][a]	11.0 [− 8.8 to 30.9][b]	0.9912

[a] 95% CI (confidence interval) of the slope.
[b] 95% CI (confidence interval) of the intercept.

Table 2
Accuracy and precision.

Compound	Conc.(mg/mL)	Mean recovery % (n = 3)	Precision RSD %(n = 3)
L-ASNase	0.396	97.9	3.2
	0.791	102.2	2.9
	1.187	104.4	1.5
Impurity 1	0.072	92.1	4.6
	0.144	98.1	2.4
	0.215	109.8	1.7
Impurity 2	0.034	96.3	1.7
	0.045	99.8	3.2
	0.068	109.7	3.8

linearity equations and R-squared values for these three calibration curves are presented in Table 1, where x and y are the concentration and the peak area of the components, respectively. The method accuracy was calculated by comparing the found concentrations (calculated from the calibration equation using the obtained peak area) with the theoretical concentrations. The accuracy and precision for L-ASNase were found to be 97.9–104.4% and 1.5–3.2% of RSD (n = 3) (Table 2) [41]. For impurity 1, accuracy and precision were 92.1–109.8% with 1.7–4.6% of RSD. For impurity 2, accuracy and precision were 96.3–109.7% with 1.7–3.8% of RSD. For L-ASNase, LOD and LOQ were 5.7 μg/mL and 18.9 μg/mL (corresponding to 0.57% [m/m] and 1.89% [m/m]), respectively. LOD and LOQ for impurity 1 and impurity 2 were identical, *i.e.* 5.7 μg/mL and 19.1 μg/mL (corresponding to 0.57% [m/m] and 1.91% [m/m]), respectively.

PBD was applied for assessing the robustness of the optimized CE-UV method, with following responses: 1) RSD (%) of p/v value (definition of the resolution can be seen in Section 3.1); 2) RSD (%) of migration time of API; 3) RSD (%) of peak area of API. The target specifications of each response were all defined to be maximal 3.0% (RSD). The experimental results of each response were all located within the specifications, which indicates a robust CE-UV method. Moreover, the significance of the regression models for these responses had been assessed by the ANOVA F-test. The p values (0.723 for RSD of p/v value, 0.948 for RSD of migration time and 0.920 for RSD of peak area of API) indicate insignificant models, which is consistent with the regression coefficients of each response (Fig. 5).

3.4. Application: modification rate

The optimal CZE-UV method is applied on L-ASNase, treated with NH_3HCO_4 for different times to give modified samples (Fig. 6**a**). External standardization was used for the quantification of the API, while the internal normalization was applied for the quantification of impurities 1–3. External standardization was used for the quantification of the API and impurities (1 and 2). In the unmodified L-ASNase, the contents of API, impurity 1 and impurity 2 were calculated to be 76.8% (RSD of 0.41%), 14.5% (RSD of 1.62%) and 4.5% (RSD of 0.84%). The API content of modified samples decreased considerably at the first 8 h (45.7%), followed by a more modest decrease from 8 h to 24 h (down to 35.6%) (Fig. 6**b**). The impurity 1 content increased steeply in the first 8 h (35.3%), after which it remained constant for 8–24 h. A pronounced increase of impurity 2 was also observed in the first 8 h, while impurity 3 increased during the 0–24 h period within limited extent.

3.5. Enzyme activity of the modified L-ASNase and specifications

The enzymatic activity of unmodified (0 h) and modified samples (incubated for 8 h, 16 h and 24 h) were determined to be 103.2% (RSD of 1.75%), 101.6% (RSD of 0.35%), 99.0% (RSD of 1.08%) and 94.5% (RSD of 0.37%) of label claim respectively. The enzyme activity of the modified *E.coli* L-ASNase (containing acidic charge variants) do not significantly differ from the unmodified *E.coli* L-ASNase.

4. Discussion

Our reported method is the first CZE-UV method for quantifying the API and acidic impurities in pharmaceutical *E.coli* L-ASNase preparations. Even in the L-ASNase monograph from the Chinese Pharmacopeia (ChP), there is no method or quality evaluation for these related impurities available [42]. Due to the hydrophobic interactions and hydrogen bonding, proteins often easily adsorb to the wall of fused silica capillaries, which results in tailing peaks, poor resolution, low recovery of the analytes and non-reproducible separations [43,44]. The adoption of an optimized but simple BGE composition (*e.g.* without additive), makes our proposed method practically very attractive. The surface

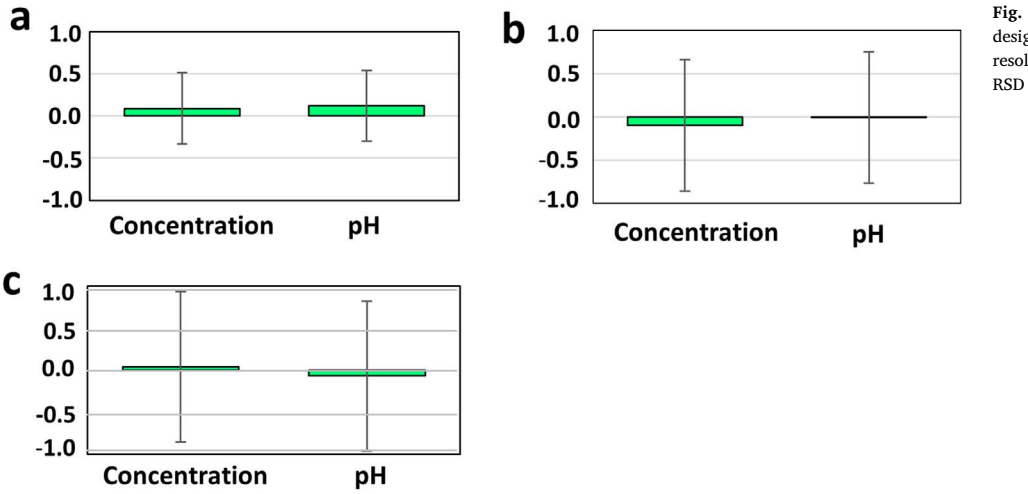

Fig. 5. Regression coefficients of Placket-Burman design (PBD) for different responses: a) RSD (%) of resolution; b) RSD (%) of migration time of API; c) RSD (%) of peak area of API.

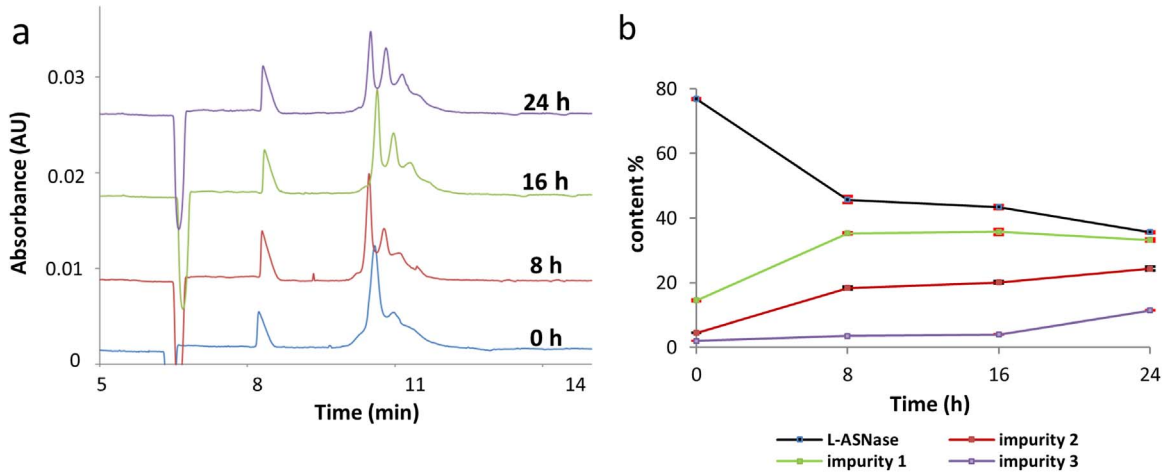

Fig. 6. Modification rate: a) electropherograms of 1.0 mg/mL modified L-asparaginase sample (incubated for 0, 8, 16 and 24 h); b) time-content curve of L-asparaginase (API) and impurity 1–3. BGE consisting of 400 mM TRIS and 400 mM boric acid (pH unadjusted, the measured pH value was pH 8.4) is applied.

silanol groups of the fused silica capillary are slightly acidic; hence are negatively charged in BGE at the applied high pH value, creating an electrical double layer with cations pulling all species towards the cathode [45]. Due to this overwhelming electroosmotic flow (EoF) and the opposite electrophoretic mobility of the more negatively charged acidic variants, the acidic variants migrate slower in the capillary moving to the cathode, compared to the native L-ASNase.

The validation results indicated that the developed CZE-UV method was selective, accurate, precise, robust and was linear in the calibration range for the API and the impurities. In the application Section 3.4.), the area normalization without factor correction was used for the quantification of the impurities (1, 2 and 3), while external standardization was used for the quantification of the API. As the responses of the impurities were close to the API (*i.e.* response factor in the range of 0.8–1.2), correction factors were not required during the internal normalization [37].

Deamidated variants are a common acidic variant occurring in the biopharmaceutical proteins [46]. The acidic species in the *Erwinia* L-ASNase was demonstrated to be deamidated species [13]. Moreover, NH_4HCO_3 induced acidic variants are deamidated species, according to previous studies [13,47]. The active, tetrameric form of L-ASNase is composed of four identical subunits. One subunit consists of two α/β domains, *i.e.* N-terminal domain and C-terminal domain (both all parallel α/β structures), connected by the linking sequence 191–212 [48]. The active site or ligand binding pocket, composed of Thr_{12}, Tyr_{25}, Ser_{58}, Thr_{89}, Asp_{90} and Lys_{162}, is located between the clefts formed by

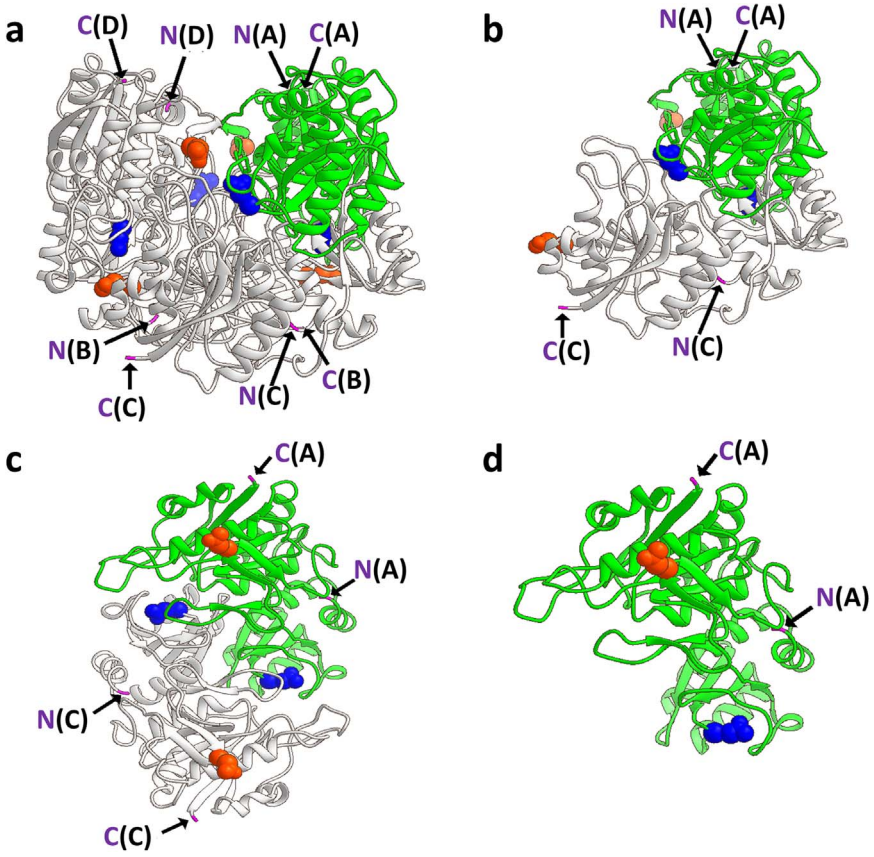

Fig. 7. Three-dimensional structure of *E.coli* L-ASNase with space fill representations of Asn_{184} in red and Asn_{246} in blue (one monomer in green and the other three monomers in grey): a) tetramer; b) dimer; c) dimer rotating 90° to the left; d) monomer. C and N represent C-terminus and N-terminus respectively, which were colored in purple. A, B, C and D in brackets represent four individual monomers, respectively. The image is created with the UCSF Chimera programme (San Francisco, USA), by using the Protein Data Bank (PDB) structure file 3ECA. (For interpretation of the references to color in this figure legend, the reader is referred to the web version of this article.)

each N-terminal domain [48,49]. The deamidation rate of Asn is influenced by the amino acid residue at the C-terminal side of Asn, with proteins and peptides with the Asn-Gly sequence showing the highest (70×) deamidation rates [50]. *E.coli* L-ASNase monomer contains 23 Asn residues, but only two Asn have a C-terminal Gly, *i.e.* Asn_{184} and Asn_{246} (Fig. 7). Asn_{184} and Asn_{246} are located in the N-terminal domain and C-terminal domain, respectively. The partially charged *E.coli* L-ASNase would be related to the Asn_{184} and Asn_{246} deamidation.

The observed slight decrease in enzyme activity of modified *E.coli* L-ASNase sample (*i.e.* 94.5% after 24 h incubation) might however not significantly influence the clinical efficacy. According to the limited clinical data, a wide range of dosages and schedules are able to achieve complete L-Asn depletion in serum and cerebrospinal fluid [51]. In addition, a relatively wide enzymatic activity specification is described in the ChP, which is currently the only Pharmacopeia including a L-ASNase monograph, *i.e.* 85–115% of label claim [42]. Clinical efficacy of *E.coli* L-ASNase preparations containing limited quantities of charge variants, as well as other aspects such as safety, remains to be further investigated to justify an appropriately quantified acceptance limit for the charge variants.

5. Conclusion

In this study, a CZE-UV method for the quantification of both the *E.coli* L-ASNase API and the acidic impurities was developed and validated using a QbD strategy. The application of L-ASNase modified samples indicated that the proposed CZE-UV approach is efficient to determine the API and the acidic impurities in the unmodified and partially modified L-ASNase. Moreover, the functional *in-vitro* enzyme activity of modified *E.coli* L-ASNase samples was evaluated, indicating an insignificant difference between the partially charged *E.coli* L-ASNase with the unmodified L-ASNase. We suggest this CZE-UV method can be adopted as a pharmaceutical quality control method.

Acknowledgment

The authors would like to thank the Ph.D. grant of the China Scholarship Council (CSC) to Han Yao (201206220137) and Xiaolong Xu (201406160087). Takeda Pharmaceutical Co., Ltd. (Brussels, Belgium) is acknowledged for supplying *E.coli* L-asparaginase preparation (Paronal®).

Appendix A. Supporting information

Supplementary data associated with this article can be found in the online version at http://dx.doi.org/10.1016/j.talanta.2018.01.048.

References

[1] C.H. Pui, L.L. Robison, A.T. Look, Acute lymphoblastic leukaemia, Lancet 371 (2008) 1030–1043.
[2] T. Maita, K. Morokuma, G. Matsuda, Amino acid Sequence of L-Asparaginase from *Escherichia coli*, J. Biochem. 76 (1974) 1351–1354.
[3] M. Ehrman, H. Cedar, J.H. Schwartz, L-Asparaginase II of *Escherichia coli*. Studies on the enzymatic mechanism of action, J. Biol. Chem. 246 (1971) 88–94.
[4] J.C. Wriston, Asparaginase: a review, Methods Enzymol. 113 (1985) 608–618.
[5] N. Bae, A. Pollak, G. Lubec, Proteins from Erwinia asparaginase Erwinase® and E. coli asparaginase 2 MEDAC® for treatment of human leukemia, show a multitude of modifications for which the consequences are completely unclear, Electrophoresis 32 (2011) 1824–1828.
[6] S. Hermeling, D.J. Crommelin, H. Schellekens, W. Jiskoot, Structure-immunogenicity relationships of therapeutic proteins, Pharm. Res. 21 (2004) 897–903.
[7] C. Plisson, M. Hunault, X. Thomas, T. Legay, Y. Bertrand, T. Andre, Y. Godfrin, L-asparaginase loaded inside red cells has an acceptable tolerability profile on bilirubin value, Blood 122 (2013) 2642.
[8] European Medicines Agency, EMA/817193/2016. 〈http://www.ema.europa.eu/docs/en_GB/document_library/Medicine_QA/2016/12/WC500218139.pdf〉 (16 December 2016).
[9] L.A. Khawli, S. Goswami, R. Hutchinson, Z.W. Kwong, J. Yang, X. Wang, Charge variants in IgG1 Isolation, characterization, in vitro binding properties and pharmacokinetics in rats, mAbs 2 (2010) 613–624.
[10] D.W. Aswad, M.V. Paranandi, B.T. Schurter, Isoaspartate in peptides and proteins: formation, significance and analysis, J. Pharm. Biomed. Anal. 21 (2000) 1129–1136.
[11] R. Gupta, O.P. Srivastava, Deamidation affects structural and functional properties of human αA-crystallin and its oligomerisation with αB-crystallin, J. Biol. Chem. 279 (2004) 44258–44269.
[12] T. Dutta, S. Banerjee, D. Soren, S. Lahiri, S. Sengupta, J.A. Rasquinha, A.K. Ghosh, Regulation of enzymatic activity by deamidation and their subsequent repair by protein L-isoaspartyl methyl transferase, Appl. Biochem. Biotechnol. 168 (2012) 2358–2375.
[13] D. Gervais, J. O'Donnell, M. Sung, S. Smith, Control of process-induced asparaginyl deamidation during manufacture of Erwinia chrysanthemil-asparaginase, Process Biochem. 48 (2012) 1311–1316.
[14] H. Svensson, Isoelectric Fractionation, analysis, and characterization of ampholytes in natural pH gradients. I. The differential equation of solute concentrations at a steady state and its solution for simple cases, Acta Chem. Scand. 15 (1961) 325–341.
[15] S. Hjerten, M. Zhu, Adaptation of the equipment for high-performance electrophoresis to isoelectric focusing, J. Chromatogr. A 346 (1985) 265–270.
[16] G. Hunt, T. Hotaling, A.B. Chen, Validation of a capillary isoelectric focusing method for the recombinant monoclonal antibody C2B8, J. Chromatogr. A 800 (1998) 355–367.
[17] J.R. Mazzeo, J.A. Martineau, I.S. Krull, Performance of isoelectric focusing in uncoated and commercially available coated capillaries, Methods 4 (1992) 205–212.
[18] J. Wu, J. Pawliszyn, Application of capillary isoelectric focusing with absorption imaging detection to the analysis of proteins, J. Chromatogr. B Biomed. Appl. 657 (1994) 327–334.
[19] X.Z. He, A.H. Que, J.J. Mo, Analysis of charge heterogeneities in mAbs using imaged CE, Electrophoresis 30 (2009) 714–722.
[20] Y. Shi, Z. Li, Y. Qiao, J. Lin, Development and validation of a rapid capillary zone electrophoresis method for determining charge variants of mAb, J. Chromatogr. B 906 (2012) 63–68.
[21] Y. He, N.A. Lacher, W. Hou, Q. Wang, C. Isele, J. Starkey, M. Ruesch, Analysis of identity, charge variants, and disulfide isomers of monoclonal antibodies with capillary zone electrophoresis in an uncoated capillary column, Anal. Chem. 82 (2010) 3222–3230.
[22] Y. He, C. Isele, W. Hou, M. Ruesch, Rapid analysis of charge variants of monoclonal antibodies with capillary zone electrophoresis in dynamically coated fused silica capillary, J. Sep. Sci. 34 (2011) 548–555.
[23] D. Gervais, Protein deamidation in biopharmaceutical manufacture: understanding, control and impact, J. Chem. Technol. Biotechnol. 91 (2016) 569–575.
[24] S. Fekete, A. Beck, J.L. Veuthey, D. Guillarme, Ion-exchange chromatography for the characterization of biopharmaceuticals, J. Pharm. Biomed. Anal. 113 (2015) 43–55.
[25] N. Bae, A. Pollak, G. Lubec, Proteins from Erwinia asparaginase Erwinase® and E. coli asparaginase 2 MEDAC® for treatment of human leukemia, show a multitude of modifications for which the consequences are completely unclear, Electrophoresis 32 (2011) 1824–1828.
[26] D. Gervais, D. King, P. Kanda, N. Foote, L. Elliott, P. Brown, N.O. Lee, K. Thalassinos, C. Pizzey, R. Rambo, T.C. Minshull, M.J. Dickman, S. Smith, Structural characterisation of non-deamidated acidic variants of Erwinia chrysanthemi L-asparaginase using small-angle X-ray scattering and ion-mobility mass spectrometry, Pharm. Res. 32 (2015) 3636–3648.
[27] D. Gervais, N. Allison, A. Jennings, S. Jones, T. Marks, Validation of a 30-year-old process for the manufacture of L-asparaginase from Erwinia chrysanthemi, Biosyst. Eng. 36 (2013) 453–460.
[28] D. Gervais, D. King, Capillary isoelectric focusing of a difficult-to-denature tetrameric enzyme using alkylurea–urea mixtures, Anal. Biochem. 495 (2014) 90–95.
[29] D. Gervais, N. Foote, Recombinant deamidated mutants of erwinia chrysanthemi l-asparaginase have similar or increased activity compared to wild-type enzyme, Mol. Biotechnol. 56 (2014) 865–877.
[30] S. Shifrin, B.J. Grochowski, L-asparaginase from Escherichia coli B. Succinylation and subunit interactions, J. Biol. Chem. 247 (1972) 1048–1054.
[31] R.L. Pérez, G.M. Escandar, Liquid chromatography with diode array detection and multivariate curve resolution for the selective and sensitive quantification of estrogens in natural waters, Anal. Chim. Acta 835 (2014) 19–28.
[32] S. Arase, K. Horie, T. Kato, A. Noda, Y. Mito, M. Takahashi, T. Yanagisawa, Intelligent peak deconvolution through in-depth study of the data matrix from liquid chromatography coupled with a photo-diode array detector applied to pharmaceutical analysis, J. Chromatogr. A 1469 (2016) 35–47.
[33] N. Brestrich, T. Hahn, J. Hubbuch, Application of spectral deconvolution and inverse mechanistic modelling as a tool for root cause investigation in protein chromatography, J. Chromatogr. A 1437 (2016) 158–167.
[34] Experimental objective: optimization, in: Analysis of factorial designs, in: L. Eriksson, E., Johansson, N. Kettaneh-Wold, C., Wikstrom, S., Wold, Design of Experiments: Principles and Applications, third revised and enlargeded., Umetrics, Umeå, 2008, pp. 145–167.
[35] O.V. Krokhin, M. Antonovici, W. Ens, J.A. Wilkins, K.G. Standing, Deamidation of -Asn-Gly- Sequences during sample preparation for proteomics: consequences for MALDI and HPLC-MALDI Analysis, Anal. Chem. 78 (2006) 6645–6650.
[36] B.M. De Spiegeleer, M. D'Hondt, E. Vangheluwe, K. Vandercruyssen, B.V. De Spiegeleer, H. Jansen, I. Koijen, J. Van Gompel, Relative response factor determination of β-artemether degradants by a dry heat stress approach, J. Pharm. Biomed. Anal. 20 (2012) 111–116.
[37] Ph. Eur. 2. 2.46 Chromatographic separation techniques, in: General chaptors,

European Pharmacopoeia, 9th Edition 2016, Volume I, Strasbourg Cedex, 2016, pp. 74–81.
[38] N. Bracke, S. Barhdadi, E. Wynendaele, B. Gevaert, M. D'Hondt, B. De Spiegeleer, Surface acoustic wave biosensor as a functional quality method in pharmaceutics, Sens. Actuators B Chem. 210 (2015) 103–112.
[39] H. Yao, J. Vancoillie, M. D'Hondt, E. Wynendaele, N. Bracke, B. De Spiegeleer, An analytical quality by design (aQbD) approach for a L-asparaginase activity method, J. Pharm. Biomed. Anal. 117 (2016) 232–239.
[40] Analysis of factorial designs, in: L. Eriksson, E., Johansson, N. Kettaneh-Wold,C., Wikstrom, S., Wold, Design of Experiments: Principles and Applications, third revised and enlarged ed., Umetrics, Umeå, 2008, pp. 75–99.
[41] ICH Guideline Q2(R1), Validation of Analytical Procedures: Text and Methodology.
[42] General monographs part 1, in: Chinese Pharmacopoeia Commission, Pharmacopoeia of the People's Republic of China Volume II, Beijing, 2010, 2010, pp. 35–38.
[43] V. Hlady, J. Buijs, Protein adsorption on solid surfaces, Curr. Opin. Biotechnol. 7 (1996) 72–77.
[44] V. Dolnik, Capillary zone electrophoresis of proteins, Electrophoresis 18 (1997) 2353–2361.
[45] H. Whatley, Basic principles and modes of capillary electrophoresis, in: J.R. Petersen, A., A. Mohammad (Eds.), Clinical and Forensic Applications of Capillary Electrophoresis, Humana Press, New Jersey, 2001, pp. 21–58.
[46] D. Gervais, Protein deamidation in biopharmaceutical manufacture: understanding, control and impact, J. Chem. Technol. Biotechnol. 91 (2016) 569–575.
[47] A. Di Donato, M.A. Ciardiello, M. de Nigris, R. Piccoli, L. Mazzarella, G. D'Alessio, Selective deamidation of ribonuclease A. Isolation and characterization of the resulting isoaspartyl and aspartyl derivatives, J. Biol. Chem. 268 (1993) 4745–4751.
[48] A.L. Swain, M. Jaskólski, D. Housset, J.K. Rao, A. Wlodawer, Crystal structure of *Escherichia coli* L-asparaginase, an enzyme used in cancer therapy, Proc. Natl. Acad. Sci. USA 90 (1993) 1474–1478.
[49] G.J. Palm, J. Lubkowski, C. Derst, S. Schleper, K.H. Rohm, A. Wlodawer, A covalently bound catalytic intermediate in *Escherichia coli* asparaginase: crystal structure of a Thr-89-Val mutant, FEBS Lett. 390 (1996) 211–216.
[50] R. Tyler-Cross, V. Schirch, Effects of amino acid sequence, buffer, and ionic strength on the rate and mechanism of deamidation of asparagine residues in small peptides, J. Biol. Chem. 266 (1991) 22549–22556.
[51] E. Ahlke, U. Nowak-Gottl, P. Schulze-Westhoff, G. Werber, H. Borste, G. Würthwein, H. Jürgens, J. Boos, Dose reduction of asparaginase under pharmacokinetic and pharmacodynamic control during induction therapy in children with acute lymphoblastic leukaemia, Br. J. Hematol. 96 (1997) 675–681.